

THE ANALYSIS OF THE EFFECTIVENESS OF THE SEISMIC NOISE ATTENUATION BY MEANS OF KARHUNEN–LOEVE (K-L) TRANSFORM

Analiza skuteczności tłumienia zakłóceń sejsmicznych za pomocą transformacji Karhunena–Loevego (K-L)

Zbigniew KASINA

*Akademia Górniczo-Hutnicza, Wydział Geologii, Geofizyki i Ochrony Środowiska,
Katedra Geofizyki; al. Mickiewicza 30, 30-059 Kraków;
e-mail: kasina@geol.agh.edu.pl*

Abstract: In the paper the analysis of the effectiveness of multiples and random noise attenuation using Karhunen–Loeve (K-L) transform is presented. The K-L transform is realized with application the process Eigenimage Filter in seismic data processing system ProMAX. The basic part of the paper is directed to the analysis of multiples attenuation by means of the K-L transform applied to field data. In the analysis the common shot point gathers (seismic records) were used as well as the traces of the CDP gathers. In the case of CDP gathers the main attention was paid on the multiple attenuation in the averaged CDP gathers (supergathers) prepared for the interactive velocity analysis. The influence of the K-L filter parameters was defined on the effectiveness of multiples removing from the velocity analysis wave images. Finally the effectiveness of the K-L filter was estimated in improving the coherent to random signals ratio on the seismic records.

Key words: geophysics, seismic method, processing, K-L transform, noise attenuation

Treść: W prezentowanej pracy przedstawiono analizę efektywności tłumienia fal wielokrotnych i szumu przypadkowego za pomocą filtracji Karhunena–Loevego (K-L), realizowanej z wykorzystaniem procedury *Eigenimage Filter* systemu przetwarzania ProMAX. Zasadniczą część pracy poświęcono analizie efektywności tłumienia fal wielokrotnych za pomocą filtracji K-L, zastosowanej do danych połowych. W analizie wykorzystano zarówno trasy kolekcji wspólnego punktu wzbudzenia (rekordy sejsmiczne), jak i trasy kolekcji wspólnego punktu odbicia (kolekcje CDP). W przypadku kolekcji CDP uwagę skoncentrowano na osłabianiu fal wielokrotnych w uśrednionych kolekcjach CDP (superkolekcje CDP), przygotowanych do interaktywnej analizy prędkości. Określono wpływ parametrów filtracji K-L na skuteczność usuwania fal wielokrotnych z obrazu fałowego analiz prędkości. W końcowym etapie pracy oceniono skuteczność filtracji K-L w poprawianiu stosunku sygnałów koherentnych do zakłóceń przypadkowych na rekordach sejsmicznych.

Słowa kluczowe: geofizyka, metoda sejsmiczna, przetwarzanie, transformacja K-L, tłumienie szumu

INTRODUCTION

Among many tools used for multiples attenuation (Weglein 1999, Kasina 2001a) the most common application in the seismic data processing systems found two transforms: F-K transform (2-D Fourier transform) and Radon transform. The Radon transform is used in two variants. The first one is based on parabolic or hiperbolic Radon transform and the second variant applies slant stack together with predictive deconvolution in the tau-p domain. The analysis of the effectiveness of the discussed transforms was the subject of many publications (e.g. Kasina 2001b, c).

The K-L transform was used not so often in practice to multiple attenuation in spite of many advantages mentioned in earlier publications (Jones & Levy 1987, Al-Yahya 1991). However it was more often applied to remove surface waves (Liu 1999, Bitri & Grandjean 2004). The latest, joined application with the wavelet transform was proposed (Kritski *et al.* 2007) as the effective tool for selection and analysis the dispersive waves.

In the presented paper the attention has been paid on the effectiveness analysis of K-L filtering realized by means of Eigenvector Filter process in the seismic data processing system ProMAX. The basic part of the paper is directed to the analysis of multiples attenuation by means of the K-L transform applied to field data. In the analysis the common shot point gathers were used as well as the traces of the CDP gathers. In the case of CDP gathers the main attention was paid on the multiple attenuation in the averaged CDP gathers (supergathers) prepared for the interactive velocity analysis. Finally, the effectiveness of the K-L filter was estimated in improving the coherent to random signal ratio on the seismic records.

K-L TRANSFORM AS O TOOL OF MULTIPLE ATTENUATION

The K-L transform applied to the seismic traces has the following form

$$\psi_j(t) = \sum_{i=1}^n a_{ij} x_i(t), \quad j = 1, \dots, n \quad (1)$$

where:

- $\psi_j(t)$ – K-L transform,
- $x_i(t)$ – input seismic traces,
- a_{ij} – transform coefficients.

The above relation may be written in the matrix form

$$\hat{\Psi} = \hat{A} \hat{X}.$$

The inverse K-L transform has the form

$$x_i(t) = \sum_{j=1}^n b_{ij} \psi_j(t), \quad i = 1, \dots, m; \quad m < n \quad (2)$$

or the matrix form

$$\hat{\Psi} = \hat{B} \hat{X} \quad (3)$$

To find the matrix coefficients of \hat{A} or \hat{B} matrix, we must perform the spectral decomposition of covariance matrix \hat{C}

$$\hat{C} = \hat{X} \hat{X}^T$$

In the spectral decomposition of matrix \hat{C} we are looking for the matrices \hat{R} and $\hat{\Lambda}$ from the matrix equation

$$\hat{C} = \hat{X} \hat{X}^T = \hat{R} \hat{\Lambda} \hat{R}^T$$

where \hat{R} is the matrix of eigenvectors of covariance matrix, $\hat{\Lambda}$ is the matrix of eigenvalues of covariance matrix. The rows of matrix \hat{A} are the normalized eigenvectors of covariance matrix, and the matrix \hat{B} is identical with matrix \hat{A} (Jones & Levy 1987). The K-L filtering relies on modification of \hat{A} matrix through the selection of its eigenvalues. The \hat{B} matrix obtained after the filtering process is used to reconstruction defined by relation (3).

The starting point of K-L transform is a creation of the covariance matrix \hat{C} . Each element C_{ij} of that matrix has the form of submatrix

$$C_{ij} = \begin{bmatrix} a_{i1} a_{j1} & a_{i1} a_{j2} & \dots & a_{i1} a_{jN} \\ a_{i2} a_{j1} & a_{i2} a_{j2} & \dots & a_{i2} a_{jN} \\ \vdots & & \ddots & \\ a_{iN} a_{j1} & a_{iN} a_{j2} & \dots & a_{iN} a_{jN} \end{bmatrix}$$

where a_{kl} is the l th sample of the k th trace. Each submatrix contains elements of cross-correlation function for different lags. In the special case of the full K-L transform only the main diagonal elements of C_{ij} matrix are non-zero. Since the main diagonal elements are the zero-lag crosscorrelations, using them alone enhances horizontally correlated events only.

The multiple suppression by means of K-L filtering is realized in the following steps:

1. in the process of velocity analysis we identify the stacking velocity and onset time of the multiples;
2. using the stacking velocity of multiples we apply normal moveout corrections (NMO) to the data achieving the flattening of the multiple arrivals;
3. we realize the K-L transform in which the energy of multiples is associated with the several greatest eigenvalues (mainly with the first principal component) ordered from the greatest to the least value;
4. in the first variant we reconstruct the NMO corrected CDP gather traces omitting several principal components of K-L transform (several greatest eigenvalues); in the second variant we reconstruct the NMO corrected multiples using only several principal components;
5. we remove the NMO corrections and additionally – in the second variant – we subtract the reconstructed multiples from the input data.

The K-L filtering may be realized in the seismic data processing system ProMAX using the process named Eigenvector Filter. That process decomposes the input set of data considered as a matrix into eigenimages through the use of eigenvectors. The sum of all eigenimages reconstructs the original data traces. The choice of which eigenimages are used in reconstruction allows us to include or exclude different types of seismic events or noise. That choice may be treated as some type of a bandpass filtering over the eigenimage range. The eigenvalues and eigenvectors defined in the process of the decomposition of the covariance matrix of input traces are arranged from the greatest value to the least one. Typically the flatter events are reconstructed using the low number eigenimages, the dipping events using the middle eigenimages, and the more random components using the higher number eigenimages. The eigenimage range 0–10% means the range of eigenvalues from the first value (the greatest one) to the value with the number defined by the product ($10\% \times$ the number of traces in data gather). The eigenimage range 85–100% means including in the filtering process only the last 15% of eigenvalues.

THE ANALYSIS OF THE MULTIPLE ATTENUATION EFFECTIVENESS ON SEISMIC RECORDS

The evaluation of the effectiveness of multiple suppression using K-L filtering has been realized on the dynamite records of land seismics in the area with strong multiples. The split-spread acquisition was used with 120 channels, 50 m receiver interval and 100 m shot interval. The typical record from the area after application True Amplitude Recovery process in the variant of removing spherical divergence is presented in figure 1. The strong multiples dominate in the record from about 2300 ms to about 5300 ms with the period about 1000 ms. These strong multiples are confirmed on the autocorrelogram (Fig. 2) of the record with applied TAR, bandpass filter (removing ground roll) and NMO (with multiple velocity) processes.

The occurrence of the strong multiples at the arrival times greater than 2000 ms was the base of the choice the design and application gates in the Eigenvector Filter process in the range of times 2000–6000 ms. The multiples were reconstructed from the record with NMO corrections (with multiple velocity) applied using the mode of Eigenvector Filter process named Output Eigen-filtered zone for the eigenimage ranges: 0–0%, 0–1%, 0–2%, 0–5%. The best reconstruction of multiples was achieved starting from the eigenimage range 0–2%. The result of multiple reconstruction for the eigenimage range 0–2% is shown in figure 3. The multiple suppression was realized using the mode of Eigenvector Filter process named Subtract Eigenimage of zone for the eigenimage ranges: 0–2%, 0–3%, 0–4%, 0–5%. The satisfying result of multiple suppression was obtained for the eigenimage range 0–4% and 0–5% as it can be seen on the filtered record and its autocorrelogram (Fig. 4) for eigenimage range 0–5%. Unfortunately the level of primaries is too low in the analysed area for greater arrival times and it is difficult to identify the primaries at the background of random noise.

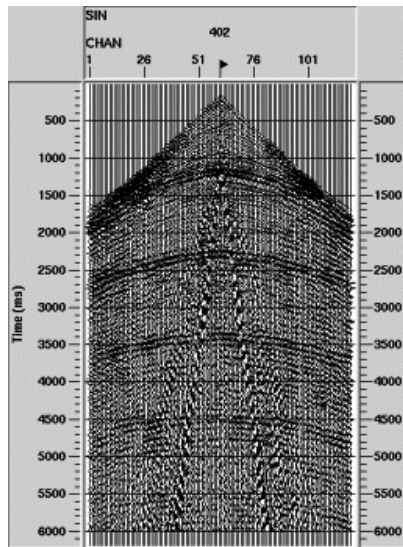


Fig. 1. The typical record from the investigated area after application TAR (True Amplitude Recovery) process in the variant of removing spherical divergence

Fig. 1. Typowy rekord z badanego obszaru po zastosowaniu procedury TAR (*True Amplitude Recovery*) w wariacie usuwania rozwierania sferycznego

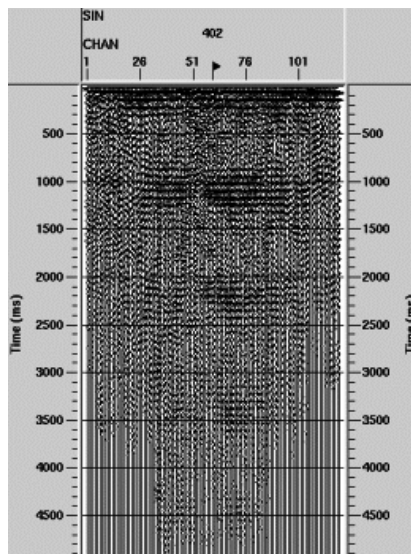


Fig. 2. The autocorrelogram of the record with applied TAR, bandpass filter (removing ground roll) and NMO (with multiple velocity) processes

Fig. 2. Autokorelogram rekordu przetworzonego za pomocą procedur TAR, filtr pasmowy (usuwiający falę powierzchniową) i NMO (z prędkością fal wielokrotnych)

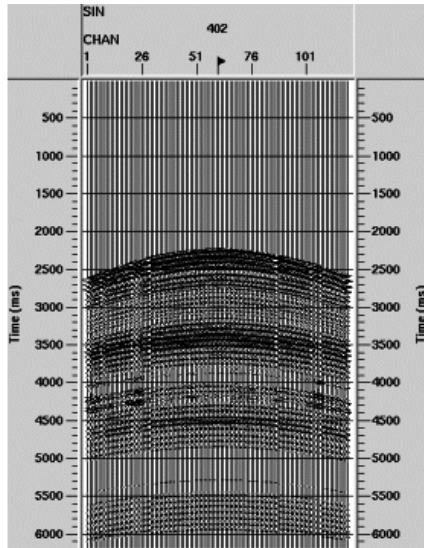


Fig. 3. The result of multiple reconstruction using the mode of Eigenvector Filter process named Output Eigen-filtered zone for the eigenimage range 0–2%

Fig. 3. Wynik rekonstrukcji fal wielokrotnych z zastosowaniem opcji procedury *Eigenvector Filter* zwanej *Output Eigen-filtered zone* dla zakresu obrazów własnych 0–2%

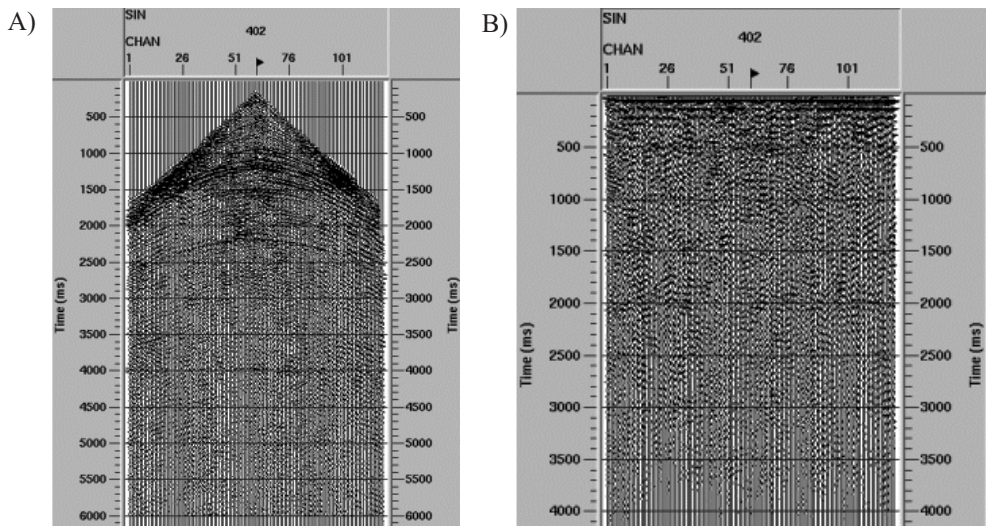


Fig. 4. The result of multiple suppression obtained for the eigenimage range 0–5% on the filtered record (A) and its autocorrelogram (B)

Fig. 4. Wynik tłumienia fal wielokrotnych uzyskany dla zakresu obrazów własnych 0–5% na poddanym filtracji rekordzie (A) i na jego autokorelogramie (B)

THE ANALYSIS OF THE MULTIPLE ATTENUATION EFFECTIVENESS IN CDP GATHERS AND IN THE VELOCITY ANALYSIS PANELS

The analysis of the multiple attenuation effectiveness in CDP gathers was realized after applying the following processing of these gathers:

- trace edition,
- TAR (removing spherical divergence),
- surface consistent spiking deconvolution,
- random noise removing (Spike&Burst Edit process),
- applying the static corrections,
- bandpass filtering (zero-phase bandpass Ormsby filter 7-12-48-60),
- creation of averaged CDP gather (Ensemble Stack/Combine process),
- applying NMO corrections with multiple velocity,
- multiple suppression using Eigenvector Filter process (mode Subtract Eigenimage of zone),
- removing NMO corrections.

The velocity of multiples were defined in the process of interactive interpretation of the results of velocity analysis. In the process of multiple suppression by means of K-L transform the CDP gathers were created by averaging 11 consecutive CDP gathers. In the analysis three representative locations of velocity analysis for considered dynamite profile were chosen. In the case of first location (CDP 402) high level of multiple amplitudes occurs. For two others locations (CDPs 602 and 802) the level of multiples is moderate. The wave patterns of the three analysed supergathers and the their Semblance panels of velocity analysis are illustrated in figures 5–7. The image of the Semblance function confirms in each case of the velocity analysis location appearing of the multiples with velocity about 2500 m/s starting from the arrival time about 1800 ms. The occurrence of these waves is clearly visible in the wave field of the supergather autocorrelograms before K-L filtering presented in the figures 8–10.

In the process of multiple reconstruction the design gate was used in the range 1800–5800 ms. The choice of the values of eigenimage range parameter was done basing on the Semblance panel of the velocity analysis realized after application the Eigenvector Filter process with different eigenimage range values (Fig. 11). The optimum value of eigenimage range was established as 0–2% for which we can observe distinct multiple suppression confirmed by the wave field of the autocorrelation function (Figs 12–14). At the same time the primary maxima of the semblance function are relatively not so much weaker for greater arrival times. The analysis of the wave field of the autocorrelograms and the semblance functions for all three supergathers confirms that the best result of multiple attenuation was achieved for the supergather 402 while the weakest result was observed for the supergather 602 (Fig. 15).

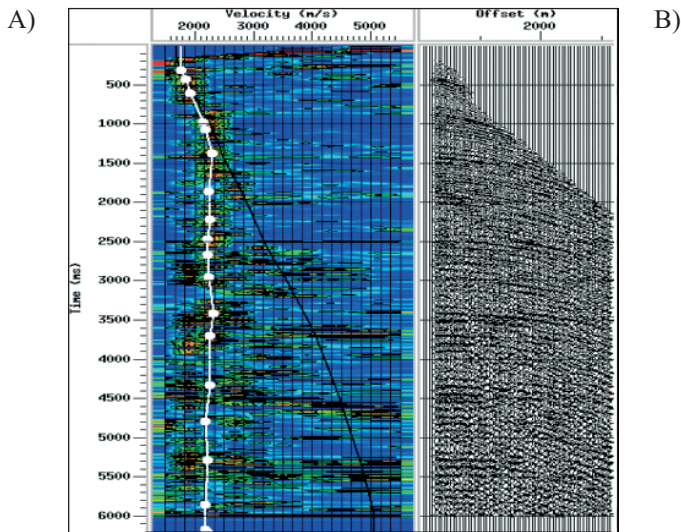


Fig. 5. The Semblance panel of velocity analysis (A) and the input supergather (B) for CDP 402 before multiple suppression with the velocity curves of primaries (black) and multiples (white) marked

Fig. 5. Panel *Semblance* analizy prędkości (A) i wejściowa superkolekcja (B) dla CDP 402 przed tłumieniem fal wielokrotnych z zaznaczonymi krzywymi prędkości fal jednokrotnych (czarna) i fal wielokrotnych (biała)

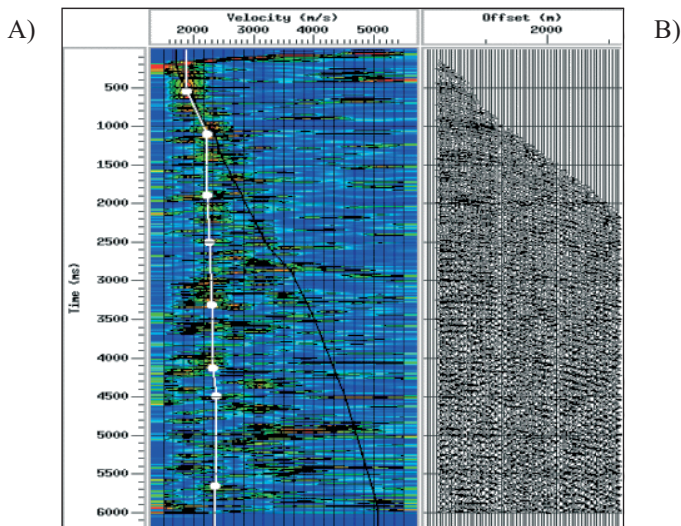


Fig. 6. The Semblance panel of velocity analysis (A) and the input supergather (B) for CDP 602 before multiple suppression with the velocity curves of primaries (black) and multiples (white) marked

Fig. 6. Panel *Semblance* analizy prędkości (A) i wejściowa superkolekcja (B) dla CDP 602 przed tłumieniem fal wielokrotnych z zaznaczonymi krzywymi prędkości fal jednokrotnych (czarna) i fal wielokrotnych (biała)

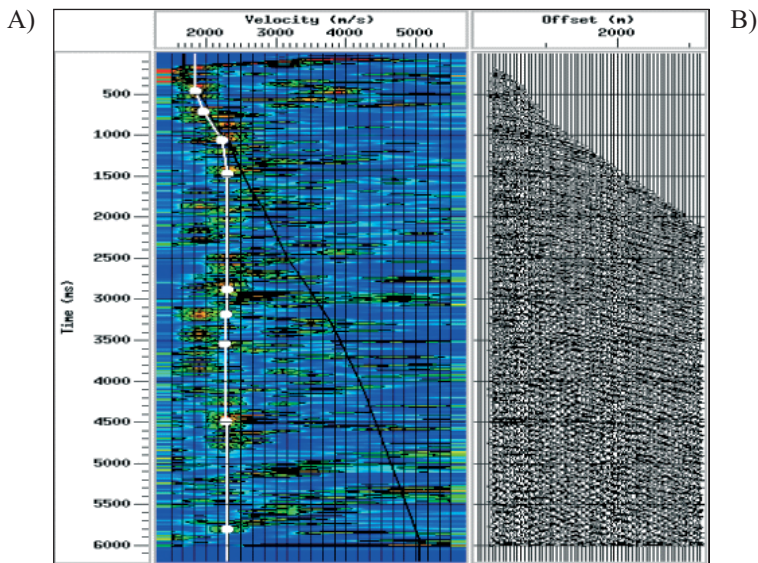


Fig. 7. The Semblance panel of velocity analysis (A) and the input supergather (B) for CDP 802 before multiple suppression with the velocity curves of primaries (black) and multiples (white) marked

Fig. 7. Panel *Semblance* analizy prędkości (A) i wejściowa superkolekcja (B) dla CDP 802 przed tłumieniem fal wielokrotnych z zaznaczonymi krzywymi prędkości fal jednokrotnych (czarna) i fal wielokrotnych (biała)

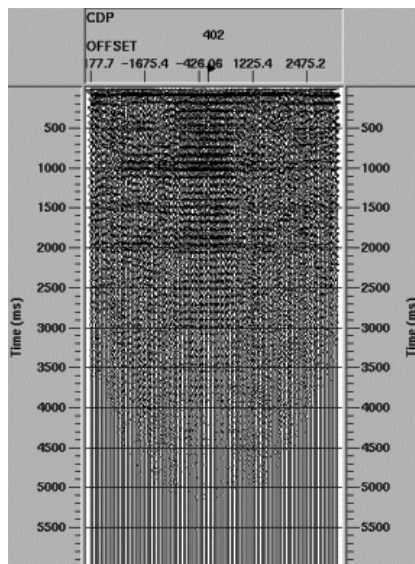


Fig. 8. The autocorrelogram of the supergather for CDP 402 before multiple suppression

Fig. 8. Autokorelogram superkolekcji dla CDP 402 przed tłumieniem fal wielokrotnych

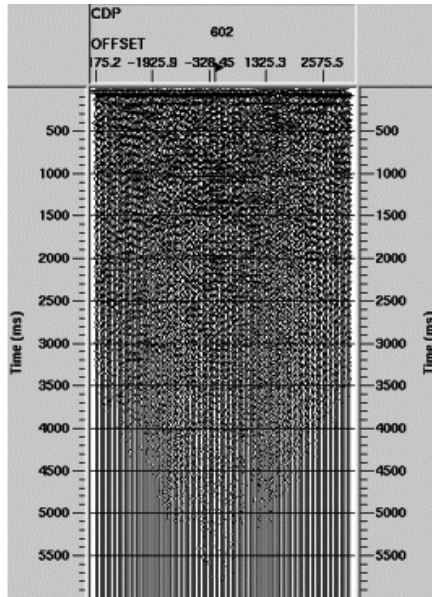


Fig. 9. The autocorrelogram of the supergather for CDP 602 before multiple suppression
Fig. 9. Autokorelogram superkolekcji dla CDP 602 przed tłumieniem fal wielokrotnych

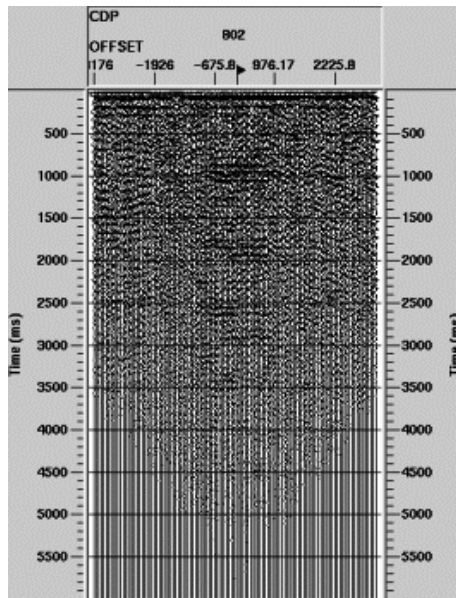


Fig. 10. The autocorrelogram of the supergather for CDP 802 before multiple suppression
Fig. 10. Autokorelogram superkolekcji dla CDP 802 przed tłumieniem fal wielokrotnych

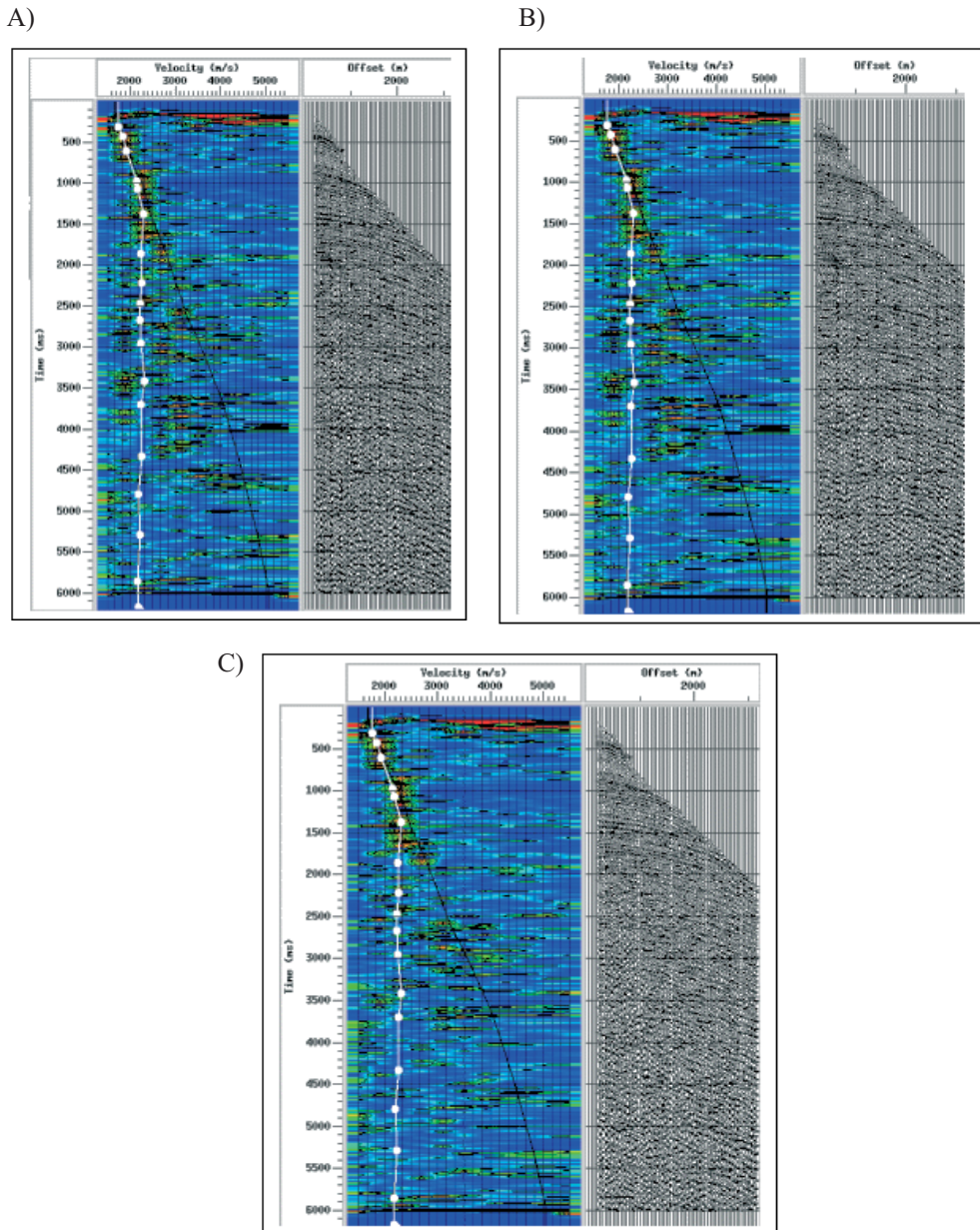


Fig. 11. The Semblance panel of velocity analysis for supergather CDP 402 after multiple suppression with the velocity curves of primaries (black) and suppressed multiples (white) marked for the eigenimage range of K-L filtering: A) 0–0%; B) 0–1%; C) 0–2%

Fig. 11. Panel *Semblance* analizy prędkości dla superpokolekcji CDP 402 po usunięciu fal wielokrotnych z zaznaczonymi krzywymi prędkości fal jednokrotnych (czarna) i osłabionych fal wielokrotnych (biała) dla zakresu obrazów własnych filtracji K-L: A) 0–0%; B) 0–1%; C) 0–2%

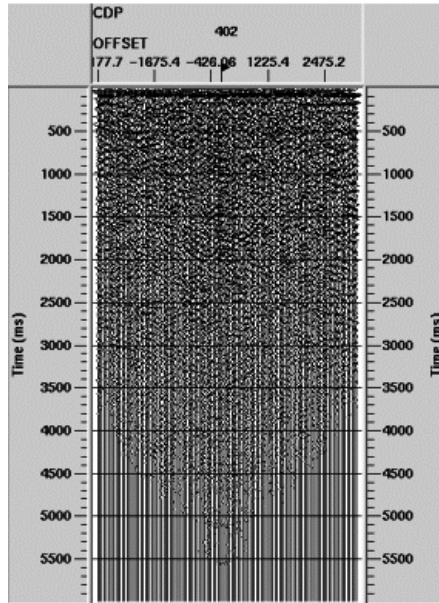


Fig. 12. The autocorrelogram of the supergather for CDP 402 after multiple suppression

Fig. 12. Autokorelogram superkolekcji CDP 402 po osłabieniu fal wielokrotnych

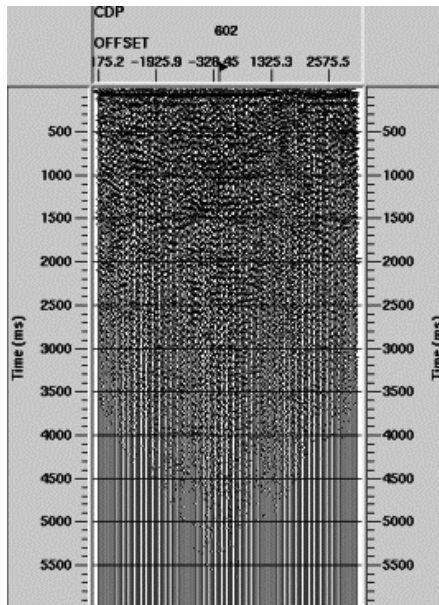


Fig. 13. The autocorrelogram of the supergather for CDP 602 after multiple suppression

Fig. 13. Autokorelogram superkolekcji CDP 602 po osłabieniu fal wielokrotnych

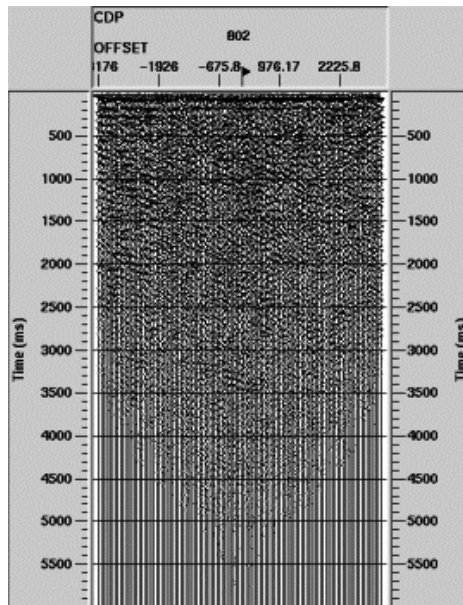


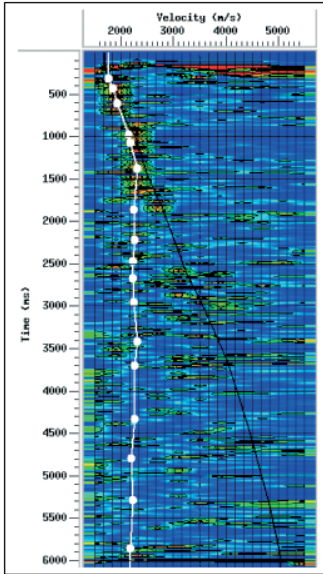
Fig. 14. The autocorrelogram of the supergather for CDP 802 after multiple suppression

Fig. 14. Autokorelogram superkolekcji CDP 802 po osłabieniu fal wielokrotnych

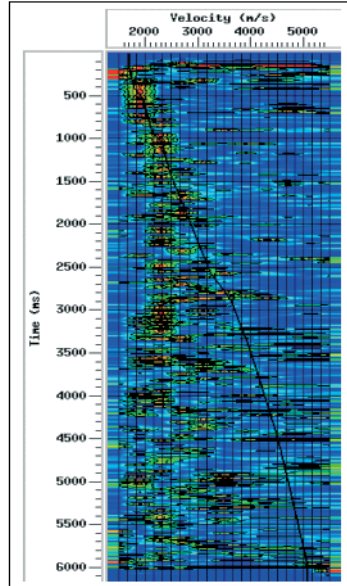
The analysis of the wave field of supergather, autocorrelograms and results of velocity analysis may it possible to formulate several conclusions referring the effectiveness of multiple suppression using K-L filtering:

- in the case when the amplitudes of primaries are significantly lower then the amplitudes of multiples the suppression of multiples using K-L transform brings out the primaries to a lower degree,
- increasing the eigenimage range enhances the effect of multiple suppression but creates the risk of decreasing the amplitudes of primaries,
- the errors of a definition of multiple velocity curve produce usually broadening applied eigenimage range and enhance the risk of decreasing of primaries in the filtered traces,
- in the considered case of the velocity distribution and the level of the reflection amplitudes the application of eigenimage range 0–2% was evaluated as the most effective,
- the multiple reconstruction gate (design gate) should include the arrival times for which multiple velocities essentially differ from the primary velocities,
- the application of the Eigenvector Filter process in the Subtract Eigenimage of zone mode (subtraction of reconstructed multiples) generates the lower risk of weakening the primaries in the process of multiple suppression than the mode Output Eigen-filtered zone,
- the analysis of the semblance function of the velocity analysis creates possibility to choice the optimum eigenimage range in the process of multiple attenuation, securing the satisfying level of primary amplitudes.

A)



B)



C)

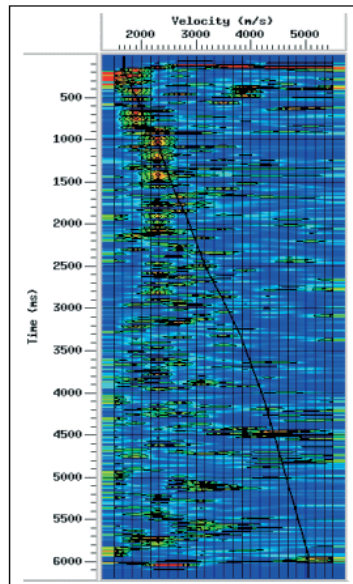


Fig. 15. The Semblance panel of velocity analysis with the velocity curves of primaries (black) and multiples (white) marked after multiple suppression for the eigenimage range of K-L filtering 0–2% for CDP supergathers: A) 402; B) 602; C) 802

Fig. 15. Panel *Semblance* analizy prędkości z zaznaczonymi krzywymi prędkości fal jednokrotnych (czarna) i wielokrotnych (biała) po usunięciu fal wielokrotnych dla zakresu obrazów własnych filtracji K-L 0–2% dla superpokolekcji CDP: A) 402; B) 602; C) 802

THE ANALYSIS OF THE RANDOM NOISE ATTENUATION EFFECTIVENESS ON SEISMIC RECORDS

The analysis of the random noise attenuation using K-L filtering (the Eigenvector Filter in the processing system ProMAX) was performed on selected dynamite record which wave field together with the random noise analysis window (design gate) is presented in figure 16. The reconstruction of the random noise was made on the record with applied nmo corrections of multiples which were the dominated reflections for arrival times greater than 1800 ms.

At the first step the reconstruction of the random noise was done using the mode Output Eigen-filtered zone for several eigenimage ranges: 80–100%, 85–00%, 90–100%. The results of that reconstruction are shown in figure 17. Only for the eigenimage range 80–100% we can identify the distinct remnant of coherent signals of the first breaks.

The wave picture of the analysed record no. 402 after TAR process applied and reconstruction using K-L filter in the mode od Subtract Eigenimage of zone (subtraction of reconstructed random noise) with the value of eigenimage range 85–100% is presented in figure 18. The decreasing of the random noise level is noticeable – in spite of high level of ground roll amplitudes – at the arrival times greater than about 3500 ms.

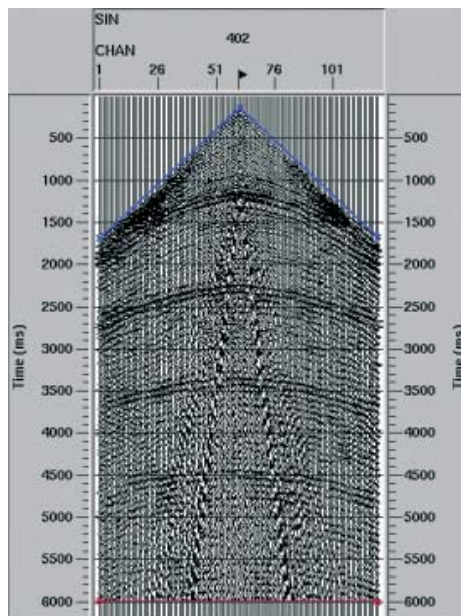


Fig. 16. The wave field of the selected dynamite record with the random noise analysis window (design gate) marked

Fig. 16. Pole falowe wybranego rekordu dynamitowego z zaznaczonym oknem (*design gate*) analizy szumu przypadkowego

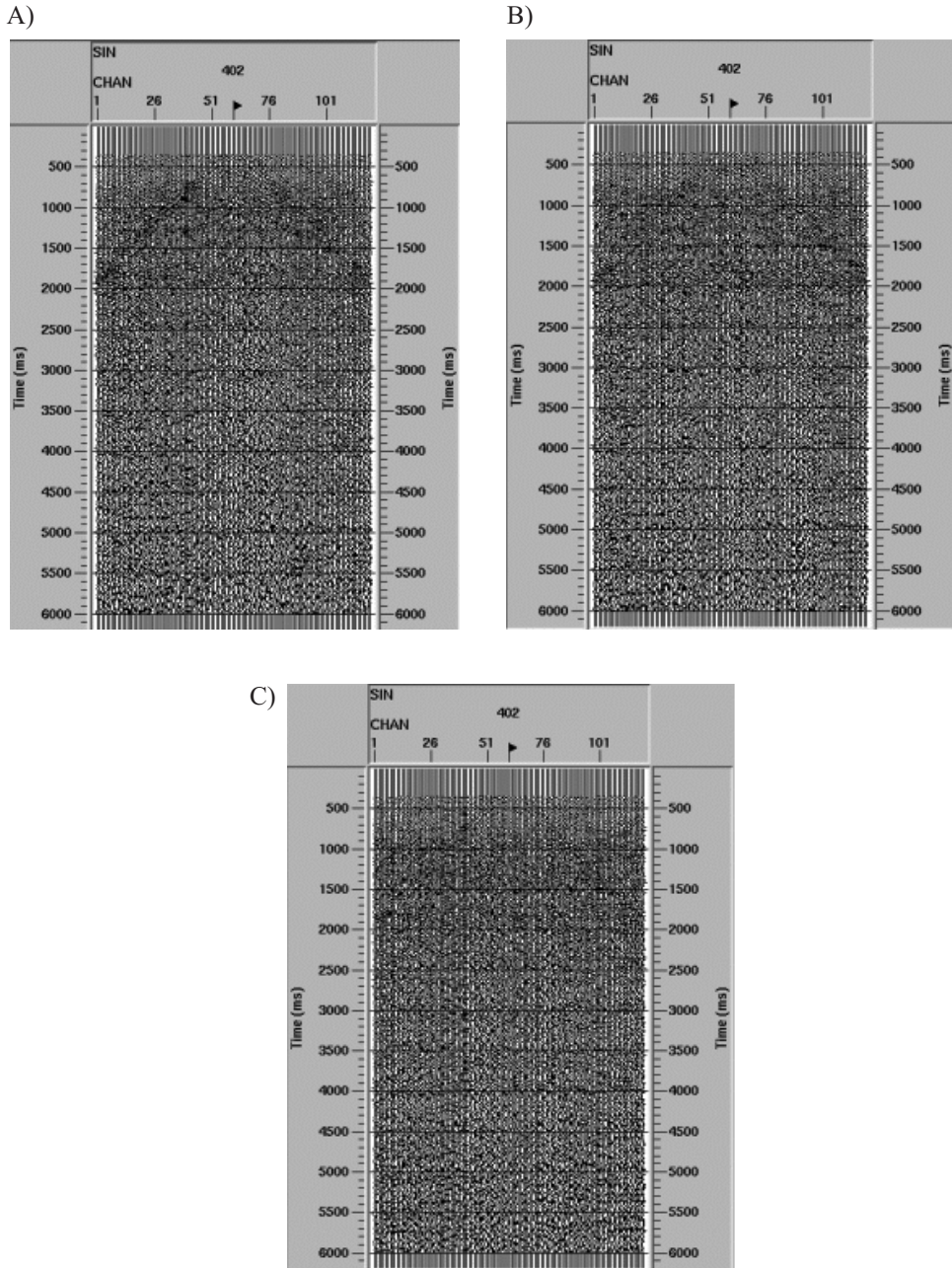


Fig. 17. The results of the random noise reconstruction using the mode *Output Eigen-filtered zone* for several eigenimage ranges: A) 80–100%; B) 85–100%; C) 90–100%

Fig. 17. Wyniki rekonstrukcji szumu przypadkowego z zastosowanie opcji *Output Eigen-filtered zone* dla kilku zakresów obrazów własnych: A) 80–100%; B) 85–100%; C) 90–100%

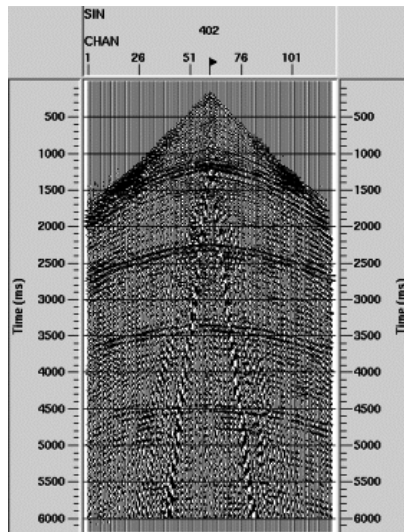


Fig. 18. The wave picture of the record no. 402 from figure 16 after its reconstruction using K-L filtering in the mode of random noise subtraction with the value of eigenimage range 85–100%

Fig. 18. Obraz falowy rekordu nr 402 z figury 16 po jego rekonstrukcji z zastosowaniem filtracji K-L w wariancie odejmowania szumu przypadkowego dla wartości zakresu obrazów własnych 85–100%

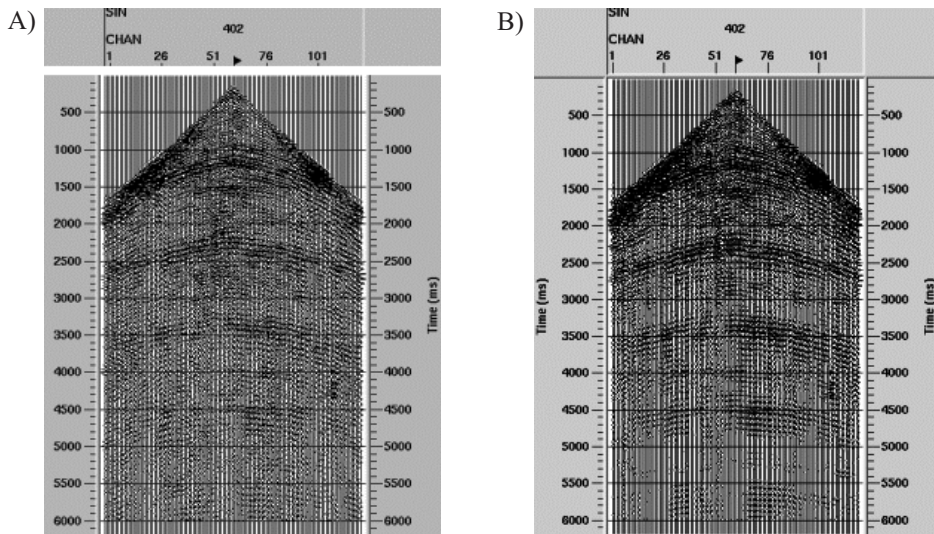


Fig. 19. The wave picture of the record no. 402 (A) after TAR and bandpass filtering 10-15-200-250 and its reconstruction (B) using K-L filtering in the mode of random noise subtraction with the value of eigenimage range 10–100%

Fig. 19. Obraz falowy rekordu nr 402 (A) po zastosowaniu procedury TAR i filtracji pasmowej 10-15-200-250 i jego rekonstrukcja (B) z zastosowaniem filtracji K-L w wariancie odejmowania szumu przypadkowego dla wartości zakresu obrazów własnych 10–100%

At the next step the strongest wave on the record – ground roll – was suppressed using bandpass ormsby filter 10-15-200-250, retaining high frequencies of random noise. The filtered record has been filtered using the mode Subtract Eigenimage of zone with much broader eigenimage ranges (10–100%, 20–100%, 30–100%, 40–100%, 50–100%) in the process of random noise reconstruction. The strongest effect of random noise suppression was confirmed for the eigenimage range 10–100% (Fig. 19). Gradual decreasing of that range from 20–100% to 50–100% did not cause strong variations of the random noise level.

CONCLUSIONS

The broad range of the realized calculations with the application of the Eigenvector Filter process in the seismic processing system ProMAX let to estimate the effectiveness of the suppression of the multiples and random noise on seismic records and in CDP gathers used in the velocity analysis. It was confirmed that the mode of noise reconstruction and subtraction from the input data may be treated as the effective tool of noise attenuation. The eigenimage range is the main parameter of K-L filtering. The optimum selection of that parameter needs the interactive analysis of the filtration results. In the case of the filtering of the CDP supergathers used in the velocity analysis as input data the choice of the optimum eigenimage range securing the satisfying multiple suppression is possible by means of the analysis of the semblance function of the velocity analysis panel. Such an analysis let us to avoid too broad expanding of eigenimage range, securing indeed the multiple attenuation but at the cost of decreasing the primary maxima of the semblance function.

The paper was prepared within the statutory works of MNiSW in Department of Geophysics, University of Science and Technology AGH, Faculty of Geology, Geophysics & Environment Protection, contract AGH no. 11.11.140.06.

REFERENCES

- Al-Yahya K.M., 1991. Application of the partial Karhunen-Loeve transform to suppress random noise in seismic sections. *Geophysical Prospecting*, 39, 77–93.
- Bitri A. & Grandjean G., 2004. Suppression of guided waves using the Karhunen-Loeve transform. *First Break*, 22, May, 45–47.
- Jones I.F. & Levy S., 1987. Signal-to-noise ratio enhancement in multichannel seismic data via the Karhunen-Loeve Transform. *Geophysical Prospecting*, 35, 12–32.
- Kasina Z., 2001a. Techniki tłumienia fal wielokrotnych w przetwarzaniu danych sejsmicznych. *Technika Poszukiwań Geologicznych, Geosynoptyka i Geotermia*, 1, 43–50.
- Kasina Z., 2001b. Analiza efektywności tłumienia fal wielokrotnych za pomocą filtracji Radona w oparciu o dane modelowe. *Technika Poszukiwań Geologicznych, Geosynoptyka i Geotermia*, 2, 45–52.

- Kasina Z., 2001c. Porównanie efektywności tłumienia fal wielokrotnych za pomocą filtracji F-K i filtracji Radona. *Geologia* (kwartalnik AGH), 27, 2–4, 562–574.
- Kritski A., Vincent A.P., Yuen D.A. & Carlsen T., 2007. Adaptive wavelets for analyzing dispersive seismic waves. *Geophysics*, 72, 1, V1–V11.
- Liu X., 1999. Ground roll suppression using Karhunen-Loeve transform. *Geophysics*, 64, 564–566.
- Weglein J.W., 1999. Multiple attenuation: an overview of recent advances and the road ahead. *The Leading Edge*, January, 40–44.

Streszczenie

W prezentowanej pracy przedstawiono analizę efektywności tłumienia fal wielokrotnych i szumu przypadkowego za pomocą filtracji Karhunena–Loevego (K-L), realizowanej z wykorzystaniem procedury *Eigenimage Filter* systemu przetwarzania ProMAX. Zasadniczą część pracy poświęcono analizie efektywności tłumienia fal wielokrotnych za pomocą filtracji K-L zastosowanej do danych polowych. W analizie wykorzystano zarówno trasy kolekcji wspólnego punktu wzbudzenia (rekordy sejsmiczne) (Fig. 1) i ich autokorelogramy (Fig. 2), jak i trasy kolekcji wspólnego punktu odbicia (kolekcje CDP). W przypadku rekordów sejsmicznych najlepszą rekonstrukcję fal wielokrotnych uzyskano, począwszy od zakresu filtracji 0–2% (Fig. 3). Zadawalający wynik tłumienia fal wielokrotnych na rekordach widoczny był w zakresie filtracji 0–5% (Fig. 4). W przypadku kolekcji CDP uwagę skoncentrowano na osłabianiu fal wielokrotnych w uśrednionych kolekcjach CDP (superkolekcje CDP) (Fig. 5–7), przygotowanych do interaktywnej analizy prędkości. Obecność silnych fal wielokrotnych potwierdzał obraz falowy autokorelogramów superkolekcji (Fig. 8–10). Określono wpływ parametrów filtracji K-L na skuteczność usuwania fal wielokrotnych z obrazu falowego analiz prędkości (Fig. 11) oraz z obrazu falowego autokorelogramów (Fig. 12–14). Analiza obrazu funkcji *Semblance* dla trzech analizowanych superkolekcji potwierdziła, że najlepszy efekt osłabiania fal wielokrotnych uzyskano w przypadku kolekcji 402, a najslabszy w przypadku kolekcji 602 (Fig. 15). W końcowym etapie pracy oceniono skuteczność filtracji K-L w poprawianiu stosunku sygnałów koherentnych do zakłóceń przypadkowych na rekordach sejsmicznych (Fig. 16–19). Najsilniejszy efekt osłabiania zakłóceń przypadkowych uzyskano w zakresie filtracji K-L 10–100% (Fig. 19).